

Selective Non-nucleoside Inhibitors of Human DNA Methyltransferases Active in Cancer Including in Cancer Stem Cells

Sergio Valente,^{†,□} Yiwei Liu,^{‡,□} Michael Schnekenburger,[§] Clemens Zwergerl,^{†,||} Sandro Cosconati,[⊥] Christina Gros,[#] Maria Tardugno,[†] Donatella Labello,[†] Cristina Florean,[§] Steven Minden,[§] Hideharu Hashimoto,[‡] Yanqi Chang,[‡] Xing Zhang,[‡] Gilbert Kirsch,^{||} Ettore Novellino,[▽] Paola B. Arimondo,[#] Evelina Miele,[○] Elisabetta Ferretti,[◆] Alberto Gulino,[◆] Marc Diederich,^{§,¶} Xiaodong Cheng,[‡] and Antonello Mai^{*,†}

[†]Dipartimento di Chimica e Tecnologie del Farmaco, Sapienza Università di Roma, P.le Aldo Moro 5, 00185 Roma, Italy

[‡]Department of Biochemistry, Emory University School of Medicine, 1510 Clifton Road, Atlanta, Georgia 30322, United States

[§]Laboratoire de Biologie Moléculaire et Cellulaire du Cancer (LBMCC), Hôpital Kirchberg, 9, rue Edward Steichen, L-2540 Luxembourg

^{||}Laboratoire d'Ingénierie Moléculaire et Biochimie Pharmacologique, Université de Lorraine—Metz, 1 Boulevard Arago, 57070 Metz, France

[⊥]DiSTABiF, Seconda Università di Napoli, Via G. Vivaldi 43, 81100 Caserta, Italy

[#]USR3388 CNRS-Pierre Fabre ETaC, CRDPF, 3 Avenue H. Curien, 31035 Toulouse Cedex 01, France

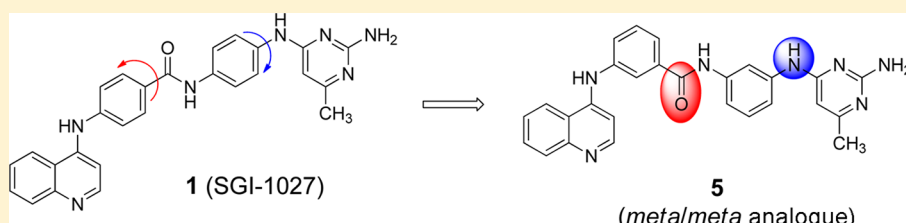
[▽]Dipartimento di Farmacia, Università di Napoli "Federico II", Via D. Montesano, 49, 80131 Napoli, Italy

[○]Istituto Italiano di Tecnologia and Dipartimento of Medicina Molecolare, Sapienza Università di Roma, Viale Regina Elena 291, 00161 Roma, Italy

[◆]Dipartimento di Medicina Sperimentale e Dipartimento di Medicina Molecolare, Sapienza Università di Roma, Viale Regina Elena 291, 00161 Rome, Italy

[¶]Department of Pharmacy, College of Pharmacy, Seoul National University, 599 Gwanak-ro, Gwanak-gu, Seoul 151-742, Korea

Supporting Information



ABSTRACT: DNA methyltransferases (DNMTs) are important enzymes involved in epigenetic control of gene expression and represent valuable targets in cancer chemotherapy. A number of nucleoside DNMT inhibitors (DNMTi) have been studied in cancer, including in cancer stem cells, and two of them (azacytidine and decitabine) have been approved for treatment of myelodysplastic syndromes. However, only a few non-nucleoside DNMTi have been identified so far, and even fewer have been validated in cancer. Through a process of hit-to-lead optimization, we report here the discovery of compound **5** as a potent non-nucleoside DNMTi that is also selective toward other AdoMet-dependent protein methyltransferases. Compound **5** was potent at single-digit micromolar concentrations against a panel of cancer cells and was less toxic in peripheral blood mononuclear cells than two other compounds tested. In mouse medulloblastoma stem cells, **5** inhibited cell growth, whereas related compound **2** showed high cell differentiation. To the best of our knowledge, **2** and **5** are the first non-nucleoside DNMTi tested in a cancer stem cell line.

INTRODUCTION

Epigenetic regulation of gene expression is mediated through at least five series of events involving changes of chromatin at the molecular level: DNA modifications, histone modifications, histone variants, noncoding RNAs, and nucleosome remodeling.^{1,2} Epigenetic control of transcription is essential to drive cells toward their normal phenotype, and epigenetic deregulation could lead to initiation and progression of human diseases

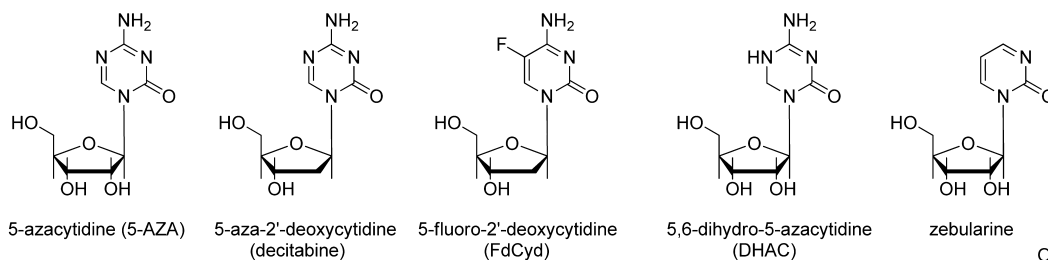
including cancer.^{3–5} In contrast to genetic origins of cancer, epigenetic aberrations are reversible events that occur at early stages in tumor genesis, and in the past decade, many interactions and connections have been reported between genetic and epigenetic changes that highlight the complex, multifactorial

Received: August 14, 2013

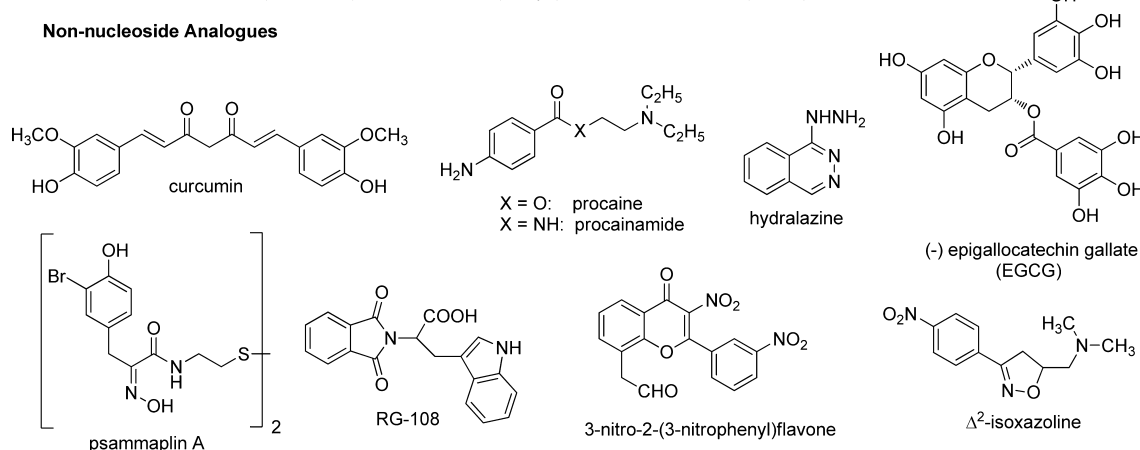
Published: January 4, 2014

Chart 1. Nucleoside and Non-nucleoside DNMT Inhibitors

Nucleoside Analogues



Non-nucleoside Analogues



nature of such disease.⁴ Among the five epigenetic events, DNA methylation has been extensively studied. Three DNA methyltransferases (DNMTs), DNMT1, DNMT3A, and DNMT3B, catalyze the transfer of a methyl group from S-adenosyl-L-methionine (AdoMet) to the C5-position of cytosine predominantly in CpG dinucleotides.^{6–9} The maintenance methyltransferase DNMT1 is most abundant in somatic cells and has a greater activity for hemi- rather than unmethylated substrates.^{8,9} Differently, de novo methyltransferase DNMT3A is only present in low amounts in somatic cells and shows no preference for hemi- or unmethylated DNA.¹⁰

In normal cells, DNA methylation plays a key role in many physiological events (genomic imprinting control, X-chromosome inactivation, maintenance of chromosomal stability, silencing of genes and endogenous retroviruses, and embryonic development), following a pattern according to which certain genomic sites are hypermethylated (gene silencing), whereas other sites, such as CpG islands, are hypomethylated (gene transcription).^{9,11} In cancer cells, aberrant DNA methylation leads to hypermethylation at CpG islands, joined to a global hypomethylation, giving rise to genomic instability and inactivation of tumor-suppressor genes.^{9,11} Hypermethylation of CpG islands is so biologically relevant and specific that for each cancer a typical hypermethylome can be drawn.¹² In addition to cancer, very recently aberrant DNA methylation has been linked to premature senescence and aging diseases such as Hutchinson–Gilford Progeria and Werner syndrome,^{13,14} to neural plasticity and GABAergic signaling modulation,^{15,16} and to heart failure and atrial fibrillation through methylation of the homeobox gene *Pitx2c*.¹⁷ Moreover, DNMT1 and DNMT3A proteins have been found to be overexpressed in rheumatoid arthritis and osteoarthritis.¹⁸

DNMT inhibitors (DNMTi) have been validated as useful tools to reactivate tumor-suppressor genes and to reprogram cancer cells toward growth arrest and death.^{9,19,20} Two nucleoside analogue DNMTi (azacytidine and decitabine, Chart 1) have

been approved by the U.S. FDA for clinical use against hematological malignancies, but despite their high efficacy, such drugs suffer from poor bioavailability, chemical instability, and toxic side effects.^{9,19} Some non-nucleoside compounds have been reported as DNMTi (Chart 1), but they typically share low potency and/or low selectivity for DNMTs, and their mechanism of inhibition is unknown.^{21–25}

Among non-nucleoside inhibitors, SGI-1027 (**1**) (Figure 1), identified among a series of quinoline-based compounds developed as anticancer drugs, has attracted our attention because of its high potency in both enzyme and cell assays.²⁶ Because the structure of **1** shows four fragments (4-aminoquinoline + 4-aminobenzoic acid + 1,4-phenylenediamine + 2,4-diamino-6-methylpyrimidine) linked in sequence with para/para orientation, we prepared a series of regioisomers of **1** by shifting each fragment's linkage from the para to the meta or ortho position (Figure 1) and obtained compounds **2–9** (Figure 1). In addition, we prepared two related compounds (**10** and **11**) showing either a bis-quinoline or bis-pyrimidine structure and two truncated compounds (**12** and **13**) lacking the “right” pyrimidine or the “left” quinoline portion, respectively (Figure 1).

■ CHEMISTRY

Compounds **1–9** were prepared by coupling the 2-, 3-, or 4-(quinolin-4-ylamino)benzoic acid, **14a–c**, with the *N*⁴-(2-, 3-, or 4-aminophenyl)-6-methylpyrimidine-2,4-diamine, **15a–c**, in the presence of benzotriazol-1-yl-oxytritypyrrolidinophosphonium hexafluorophosphate (PyBOP) and triethylamine in dry *N,N*-dimethylformamide as solvent (Scheme 1). Intermediate compounds **14a–c** were prepared by reaction between 4-chloroquinoline with the appropriate ethyl 2-, 3-, or 4-aminobenzoate and 37% hydrochloric acid in ethanol at 80 °C. The obtained ethyl benzoates, **16a–c**, underwent basic hydrolysis using 2 N potassium hydroxide to afford the corresponding acids, **14a–c**. The same reaction conducted

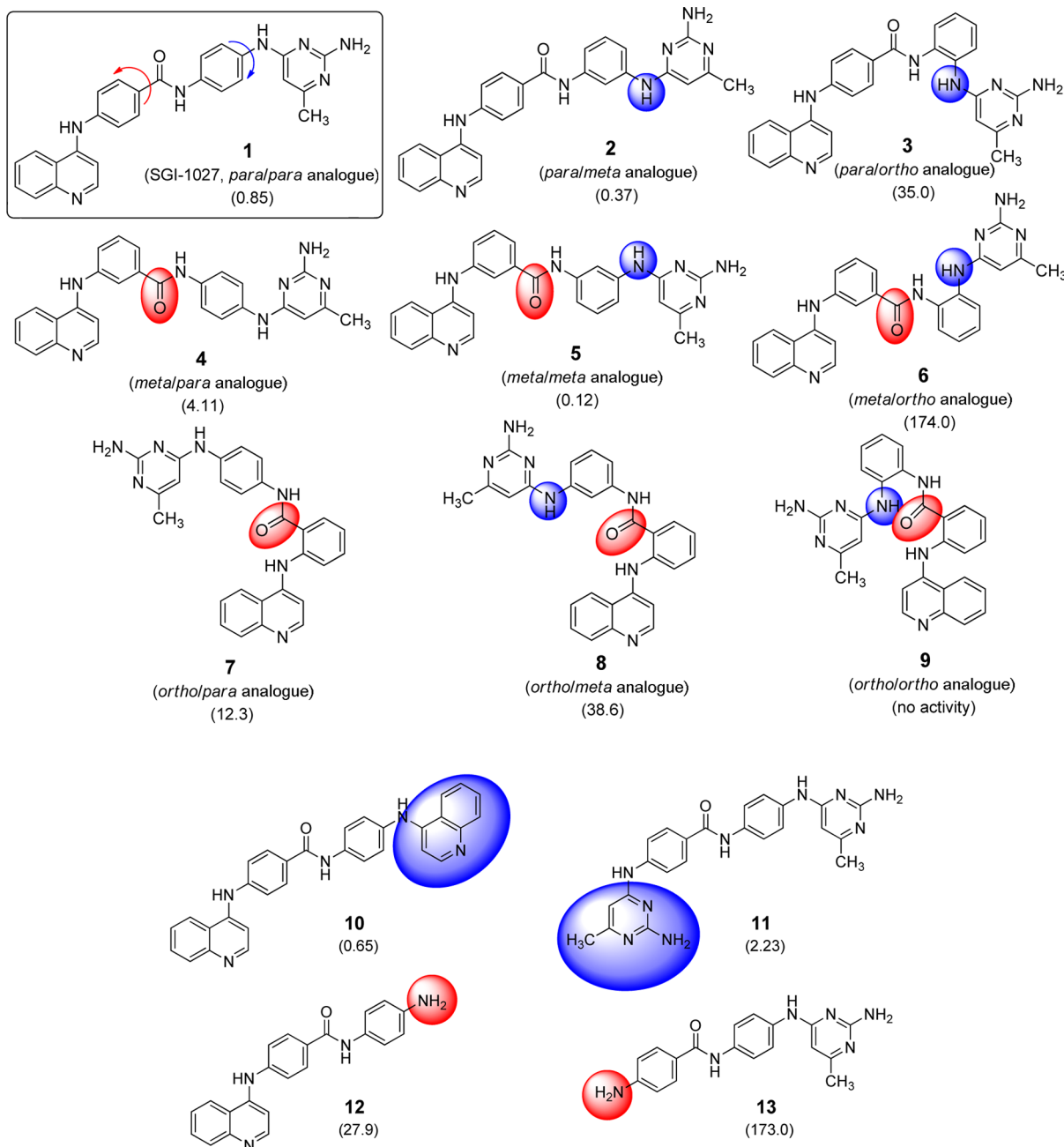


Figure 1. Chemical structures of SGI-1027 (**1**) and related analogues **2–13** described in this study. Their IC_{50} values (μM) from nanoscale HTS against human DNMT1 are reported in the brackets.

with 4-chloro-6-methylpyrimidin-2-amine and the opportune 2-, 3-, or 4-nitroanilines in the presence of 37% hydrochloric acid and ethanol at 80 °C furnished the nitro-intermediates, **17a–c**, which were in turn reduced with stannous chloride dihydrate and 37% hydrochloric acid in ethanol to the corresponding anilines, **15a–c**.

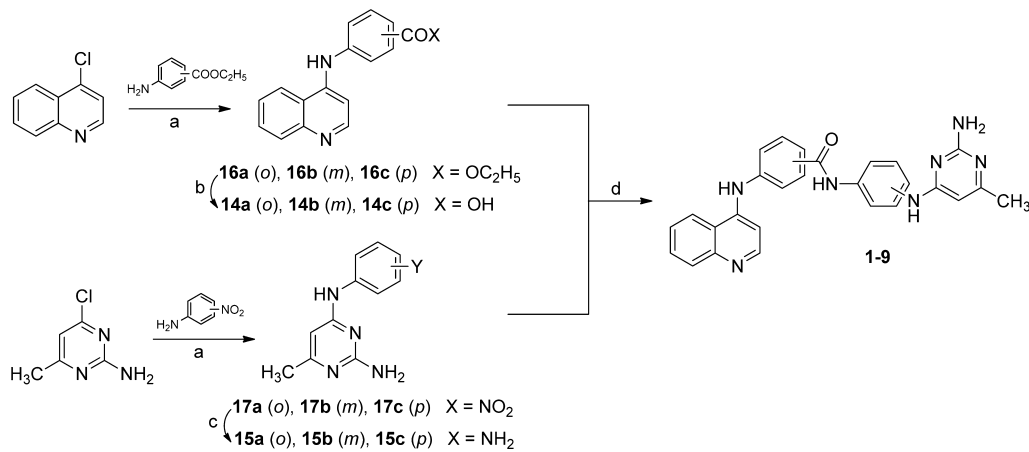
Chemical and physical data of final compounds **1–13** (Table S1) as well as those of intermediate compounds **14–22** (Table S2) are listed in the Supporting Information.

Bisquinoline **10** was obtained by treating 4-chloroquinoline with 4-nitroaniline and, after reduction of the nitro group of the resulting intermediate **18** to the corresponding aniline **19**, by coupling **19** with **16c** (Scheme 2A). Treatment of 4-chloro-6-

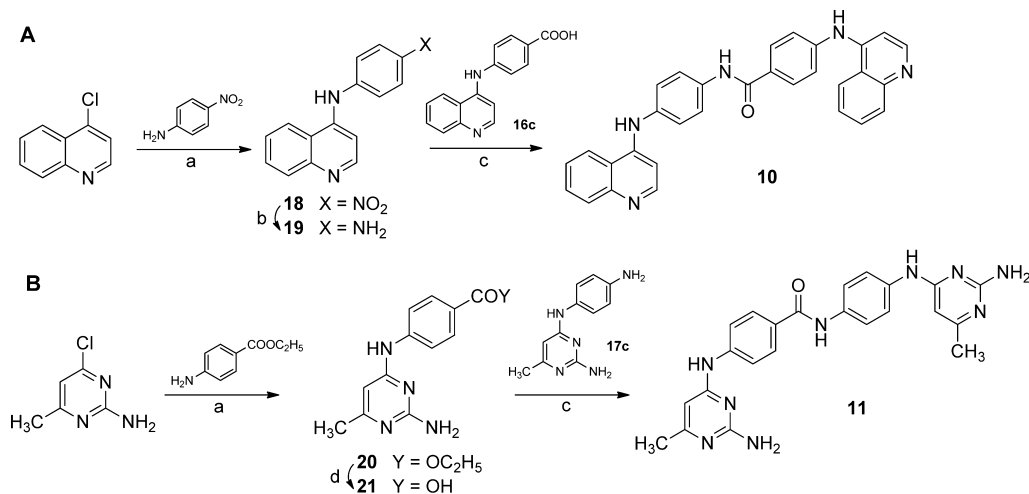
methylpyrimidin-2-amine with ethyl 4-aminobenzoate afforded intermediate ester **20**, which was hydrolyzed to acid **21** and was then coupled with **17c** to furnish bispyrimidine **11** (Scheme 2B). Truncated compounds **12** and **13** were prepared by reaction of **16c** with 4-phenyldiamine (**12**) or by reaction of **17c** with 4-nitrobenzoic acid and subsequent reduction of the nitro group of intermediate **22** to the corresponding amine (**13**) (Scheme 3).

RESULTS AND DISCUSSION

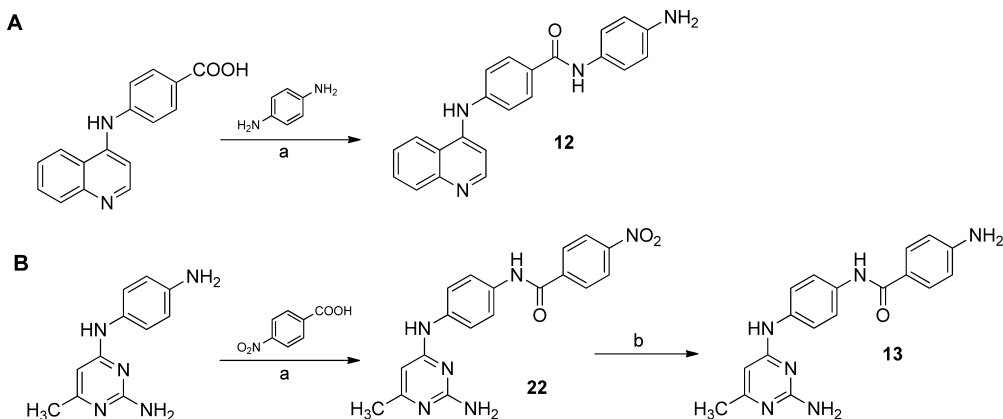
DNMT1, DNMT3A2/3L, PRMT1, and GLP Inhibition Assays. From a nanoscale prescreen performed on **1–13** against human

Scheme 1. Synthesis of Compounds 1–9^a

^aReagents and conditions: (a) 37% HCl, CH₃CH₂OH, 80 °C, 2 h; (b) 2 N KOH, CH₃CH₂OH; (c) stannous chloride dihydrate, 37% HCl, CH₃CH₂OH, 1 h, 80 °C; (d) (C₂H₅)₃N, PyBOP, anhydrous DMF, N₂ atmosphere, room temperature, 1 h.

Scheme 2. Synthesis of Compounds 10 and 11^a

^aReagents and conditions: (a) 37% HCl, CH₃CH₂OH, 80 °C, 2 h; (b) stannous chloride dihydrate, 37% HCl, CH₃CH₂OH, 80 °C, 1 h; (c) (C₂H₅)₃N, PyBOP, anhydrous DMF, N₂ atmosphere, room temperature, 1 h; (d) 2 N KOH, CH₃CH₂OH.

Scheme 3. Synthesis of Compounds 12 and 13^a

^aReagents and conditions: (a) (C₂H₅)₃N, PyBOP, anhydrous DMF, N₂ atmosphere, room temperature, 1 h; (b) stannous chloride dihydrate, 37% HCl, CH₃CH₂OH, 80 °C, 1 h.

DNMT1 using poly(dI-dC) as substrate, compounds 2, 4, and 5, obtained by replacing either or both the para with the meta

linkages in the structure of 1, emerged as highly efficient DNMT1 inhibitors, whereas the ortho regioisomers were less

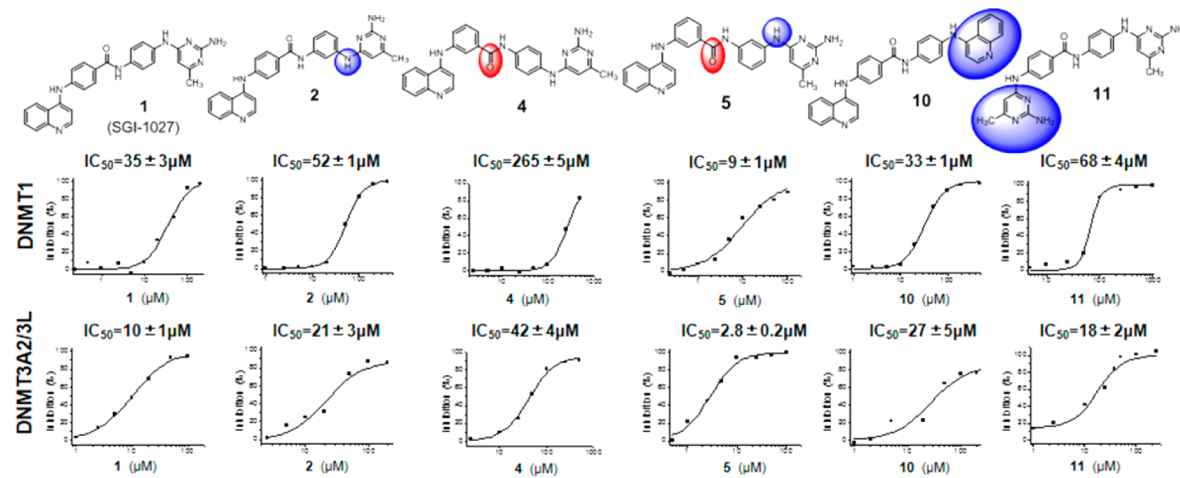


Figure 2. Inhibitory activities of **1**, **2**, **4**, **5**, **10**, and **11** against human DNMT1 (hemimethylated substrate) and the DNMT3A2/DNMT3L complex (unmethylated substrate).

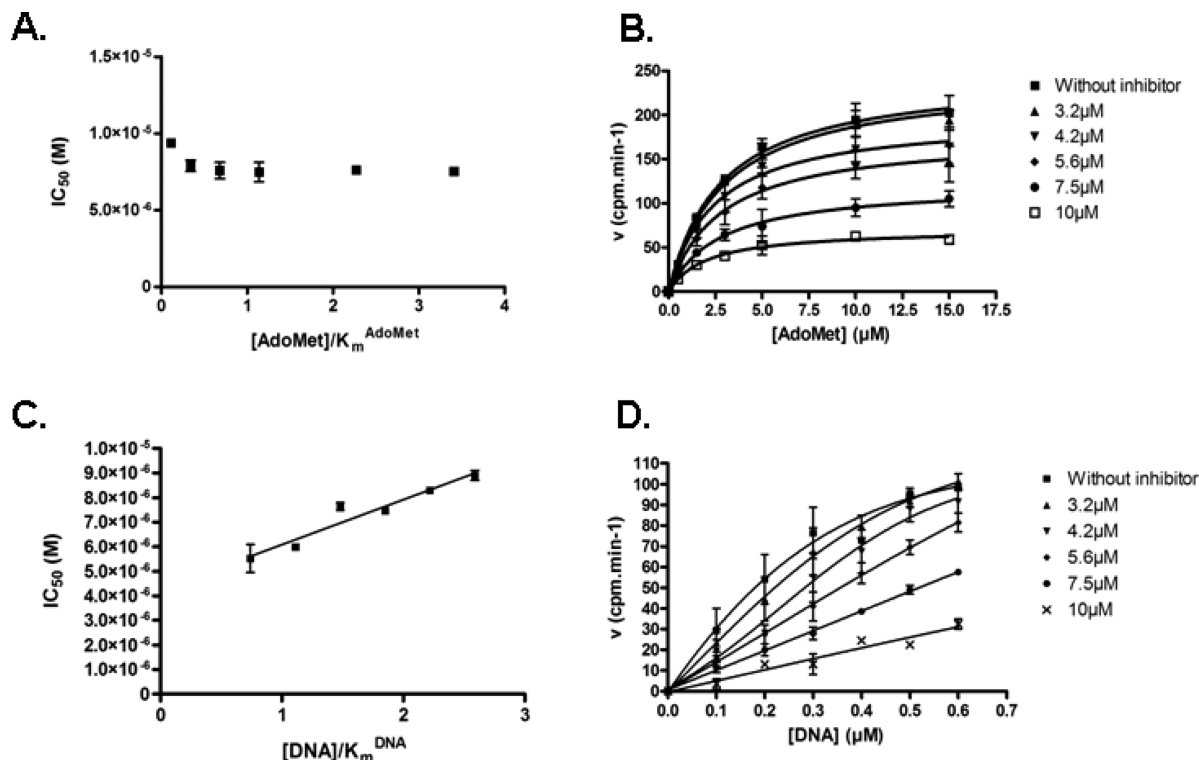


Figure 3. Competition experiments performed with compound **5** on DNMT1 by varying AdoMet concentrations at a near-saturating DNA concentration (**A, B**) or by varying DNA concentrations at a near-saturating AdoMet concentration (**C, D**). (**A**) IC₅₀ of compound **5** plotted against [AdoMet]/K_m^{AdoMet}. (**B**) Velocity plot against [AdoMet] for different concentrations of compound **5**. The lines represent the nonlinear regressions by the Michaelis-Menten equation. (**C**) IC₅₀ of **5** plotted against [DNA]/K_m^{DNA}. The line represents the linear regression. (**D**) Velocity plot against [DNA] for different concentrations of **5**. The lines represent the nonlinear regressions with sigmoidal dose-response. On each graph, the mean of two independent experiments is represented ± SEM.

potent (**3** and **6–8**) or totally inactive (**9**). Bisquinoline **10** displayed a similar potency as **1** against DNMT1, whereas bispyrimidine **11** was slightly less efficient, and truncated compounds **12** and **13** showed a severe drop in inhibition (Figure 1).

To perform a more wide and accurate inhibition assay against DNMTs, we tested the most potent compounds, **2**, **4**, **5**, **10**, and **11**, in comparison with **1** against human DNMT1 using a hemimethylated substrate and against the human DNMT3A2/DNMT3L complex using an unmethylated substrate (Figure 2). Under these assay conditions, meta/meta analogue **5** (IC₅₀ = 9 μM)

displayed a 4-fold higher activity than **1** against DNMT1, whereas the para/meta (**2**) and meta/para (**4**) analogues were 1.5- and 7.6-fold less potent, respectively. Bisquinoline **10** showed the same DNMT1 inhibiting activity as **1**, whereas bispyrimidine **11** was 2-fold less potent.

Against DNMT3A2/DNMT3L, all of the inhibitors were more efficient than against DNMT1, and **5** was again the most potent, with IC₅₀ = 2.8 μM [IC₅₀ (**1**) = 10 μM]. Among the remaining compounds, **11** and **2** were 2-fold, **10** was 3-fold, and **4** was 4-fold less potent than **1** (Figure 2).

To determine the mechanism of DNMT1 inhibition by compound **5**, we carried out competition experiments by varying the concentration of either AdoMet or DNA, and we used both the IC_{50} and the velocity plot methods to analyze the data. As shown in Figure 3, the IC_{50} analysis of **5** against the AdoMet concentration shows nearly constant IC_{50} values as the AdoMet concentration increases (Figure 3A,B), suggesting a non-competitive inhibition.²⁷ Differently, the IC_{50} of **5** increases linearly with DNA concentration, suggesting a DNA-competitive behavior (Figure 3C,D).²⁷ The velocity plot against DNA concentration displays sigmoidal deformations. These deformations have been described by Copeland and Horiuchi²⁸ and are explained by potential nonspecific substrate–inhibitor interactions (DNA interactions), tight-binding, or a time-dependent inhibitor.²⁸ Competition studies performed on structurally different compound **11** gave similar results (Figure S1 in the Supporting Information).

To determine the specificity of **1**, **2**, **4**, **5**, **10**, and **11** for DNMTs among other AdoMet-dependent enzymes, we tested them against PRMT1, a protein arginine methyltransferase,²⁹ and G9a-like protein (GLP), a histone H3 lysine 9 methyltransferase.^{30,31} Under the tested conditions, the new derivatives showed very low (if any) PRMT1- and GLP-inhibiting activities, resulting in the tested compounds being more DNMT-selective than **1**, which displayed only 4- and 1.9-fold lower activities against PRMT1 and GLP, respectively, when compared with DNMT1 inhibition. In contrast, **5** was 33- and 11-fold less potent against PRMT1 and GLP than against DNMT1 (Table 1).

Table 1. Inhibitory Activities of **1, **2**, **4**, **5**, **10**, and **11** against PRMT1 and GLP^a**

compound	PRMT1		GLP	
	IC_{50} (μ M)	DNMT1 selectivity	IC_{50} (μ M)	DNMT1 selectivity
1	139	4.0	65	1.9
2	300	5.8	600	11.5
3	300	1.1	400	1.5
4	300	33.3	100	11.1
5	100	3.0	100	3.0
6	>1000	>14.7	500	7.3

^aThe DNMT1 selectivity (as the PRMT1 or GLP/DNMT1 IC_{50} ratio) for each compound is reported. Inhibition assays were performed in duplicate. The errors in the determinations of IC_{50} 's are within $\pm 20\%$ of their values.

Docking Studies of Compound 5 in DNMT1 Structures. To delineate better the mechanism(s) for the inhibitory potency of **5** against DNMT1, molecular modeling studies were performed. In particular, compound **5** was docked in two different DNMT1 structures available in the Protein Data Bank (PDB): DNMT1 (residues 600–1600) crystallized in complex with

sinefungin (PDB 3SWR, Hashimoto and Cheng, unpublished data) and DNMT1 (residues 646–1600) in complex with both AdoHcy and a 19 bp DNA duplex (PDB 3PTA).³² These two DNMT1 structures share a similar overall 3D arrangement, with some conformational differences mainly in the DNA-binding CXXC domain region (residues 646–692, Figure S2 in the Supporting Information). The latter is adjacent to the methyltransferase domain, which is the putative inhibitor binding site, and in principle its conformation could influence the inhibitor binding. Therefore, we decided to dock **5** in both of the aforementioned structures by employing the Glide program of the Schrödinger package.³³

Docking results achieved on the DNMT1 structure alone (unbound to DNA) revealed that in the lowest-energy binding conformation (docking score -6.95) **5** should be able to span between the AdoMet binding site and the CXXC region (Figure 4).

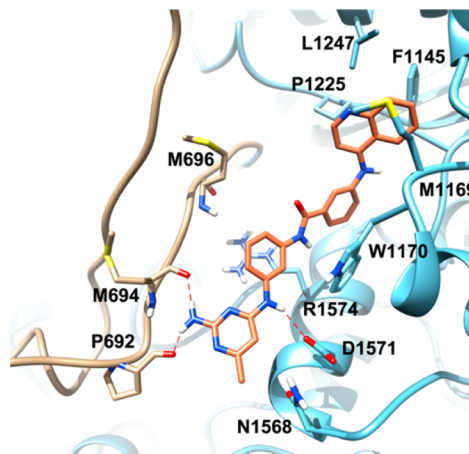


Figure 4. Predicted binding mode of **5** in the DNMT1 structure unbound to DNA (PDB 3SWR). Compound **5** is depicted as orange sticks, and the enzyme catalytic and CXXC domains are depicted as cyan (right side) and brown (left side) ribbons and sticks, respectively. H-bonds are depicted as dashed red lines.

Indeed, changing one or both the para/meta linkages (**1**, **2**, **4**, and **5**) with ortho ones (**3** and **6–9**) by modifying the ligand shape from a stretched to a more condensed one should prevent the ligand from spanning between the two sites, explaining why the presence of ortho linkages is not productive in terms of inhibitory potency. As depicted in Figure 4, the 4-aminoquinoline fragment of **5** is embedded in a lipophilic region normally occupied by the AdoMet adenine ring, establishing hydrophobic contacts with I1167, M1169, P1225, and I1247 as well as a T-shaped interaction with F1145. In this position, substitution of the quinoline ring with a smaller pyrimidine one (**11**) or with a hydrogen (**13**) would cause a partial loss of the interactions within the aforementioned cleft, thus explaining the drop in inhibitory potency. Also, the attached central fragment (3-aminobenzoic acid + 1,3-phenylenediamine) of **5** is embedded in a region in which cation–π and π–π interactions are established with R1574 and W1170, respectively. The intrinsic rigidity of this fragment allows to project the 2,4-diamino-6-methylpyrimidine terminal at the crevice between the CXXC and methyltransferase domains. In this position, the terminal hydrophilic head of **5** forms three H-bonds with the M694 and P692 backbone CO and with the D1571 side chain. Given the critical role of the CXXC region for the DNMT1 enzymatic activity,³⁴ it might be speculated that favorable ligand interactions with this region

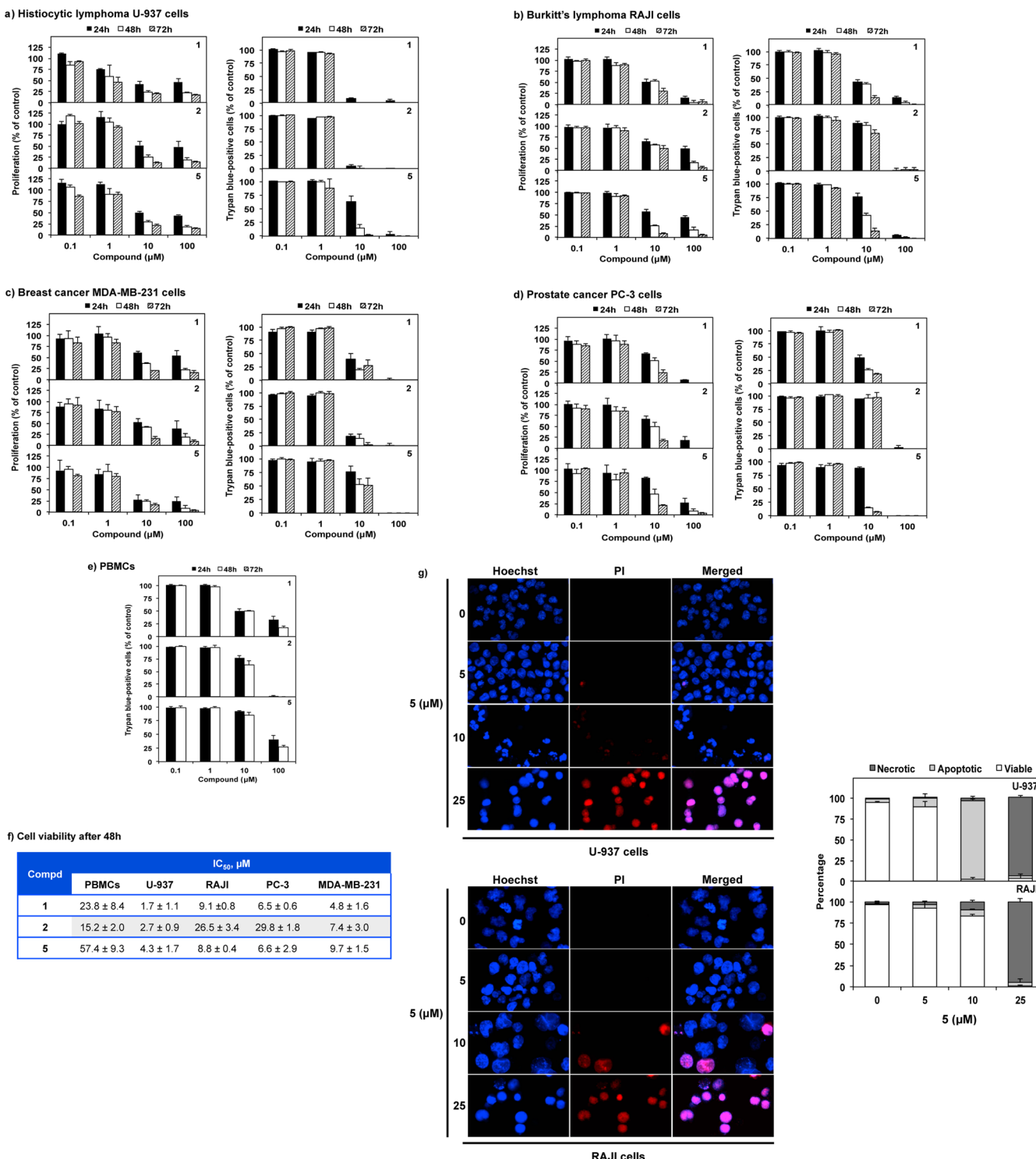


Figure 5. Cellular studies on quinoline-based DNMTi. (a–e) Antiproliferative effects (left) and cell-death induction (right) of **1**, **2**, and **5** on U-937 (a), RAJI (b), MDA-MB-231 (c), PC-3 (d), and PBMC (e) cells. (f) IC₅₀ values of cell viability relative to the above cells treated with **1**, **2**, and **5** for 48 h. (g) Nuclear-morphology analysis after Hoechst and PI staining in U-937 and RAJI cells treated with increasing doses of **5** for 72 h. Data represent the mean (\pm SD) of at least three independent experiments. Pictures are representative of three independent experiments.

should also be critical for inhibitory potency, thus explaining why replacement of the 2,4-diamino-6-methylpyrimidine (**5**) fragment with a quinoline (**10**) one or with an hydrogen (**12**) does not enhance DNMT1 inhibition.

Interestingly, the same calculations did not succeed in suggesting a well-defined binding pose for compound **5** in the enzyme/DNA structure. Indeed, in the DNMT1/DNA complex, when

merging the coordinates of **5** achieved in the absence of DNA, it seems clear that the subtle rearrangements of the CXXC domain induced by the presence of DNA would sterically hamper **5** from spanning from the AdoMet interaction site to the crevice between the CXXC and methyltransferase domains (Figure S4b in the Supporting Information). Results of analogous docking studies performed on **1** are reported in the Supporting Information

(Figures S3 and S4a). Almost the same binding orientations were obtained either in the free DNMT1 or in the DNMT1/DNA structure, suggesting that, whereas **5** can in principle be recognized by the DNA-unbound enzyme conformation (i.e., in a DNA-competitive binding mode), **1** should be able to bind DNMT1 independently from the presence of DNA.

Competition experiments also outline that the inhibitory potency of **5** is not affected by increasing concentrations of the AdoMet cofactor. These data might suggest that either the ligand is also able to adapt to binding sites that are different from that of the cofactor or the same compound can also bind the enzyme/cofactor complex. In this respect, the DNMT1 structures (PDB 3PTA and 3SWR) were also searched for different binding sites with the SiteMap software available within the Maestro suite.³³ Results of these predictions demonstrate that the most probable site is the one occupied by the cofactor, whereas four additional less probable sites could exist (Figure S5a). Nevertheless, when Glide was employed to predict a possible binding position of **5** in these enzyme regions, weak binding affinities were predicted (docking scores below 5.0), mainly because the selected clefts, being rather shallow and solvent-exposed, are less prone to provide efficient ligand interactions. This would suggest that the highest affinity DNMT1 binding site is the cofactor one. We then attempted to dock **5** in the DNMT1/AdoHcy (mimicking AdoMet substrate analogue) complex to probe whether the ligand is still able to bind this complex. Indeed, these studies suggest that in the presence of the cofactor the ligand would still positively interact with the enzyme complex, adopting a conformation (docking score -6.76, Figure S5b) in which the ligand is sandwiched between the substrate and part of the enzyme CXXC domain region (residues 646–650). This might rationalize why increasing AdoMet concentrations do not abrogate the ligand inhibition efficiency.

Effects of Quinoline-Based DNMTi in a Panel of Cancer Cell Lines.

To study the effects of these DNMTi in a cellular context, we tested **1**, **2**, **4**, **5**, **10**, and **11** in a panel of cancer cells (histiocytic lymphoma, U-937; breast cancer, MDA-MB-231; Burkitt's lymphoma, RAJI; and prostate cancer, PC-3). Trypan blue exclusion assays were carried out to determine their effects on cell proliferation and viability. The effect of the tested compounds in peripheral blood mononuclear cells (PBMCs) was also determined to assess for differential toxicity. In full agreement with their DNMT-inhibition potency, compounds **1**, **2**, and **5** displayed the highest antiproliferative effects and the strongest cell-death induction in all of the cancer cells tested (Figure 5a–d). Compounds **4**, **10**, and **11** showed both lower activity and cytotoxicity in these assays (Figure S6 in the Supporting Information). Compounds **1** and **5** showed comparable potency against tumor cells, but **5** was the less toxic in PBMCs (Figure 5e,f). Nuclear morphological changes were further observed by fluorescence microscopy after Hoechst and propidium iodide (PI) staining in both U-937 and RAJI cells treated with increasing doses of **5** to assess the levels of necrosis and apoptosis induced by the compound (Figure 5g). In U-937 cells, **5** displayed massive apoptosis at 10 μM followed by necrosis at 25 μM, whereas in RAJI cells, **5** mainly led to necrosis at 25 μM without triggering any apoptotic response at lower concentrations.

Effects of **2** and **5** in Medulloblastoma Stem Cells (MbSCs).

DNA methylation also plays a key role in cancer stem cells: A comparison of the epigenomes of normal and cancer stem cells and pluripotent and differentiated states revealed a clear link between DNMTs and transcribed loci.³⁵ In cancer stem cells, the effect of DNMT inhibitors has been poorly investigated.

Azacytidine has been shown to reactivate *SALL4* expression and transcription in acute promyelocytic leukemia NB4 cells³⁶ as well as in colorectal cancers³⁷ through DNMT inhibition. In IDH1 mutant glioma cells, decitabine induced a dramatic loss of stemlike properties and efficient adoption of markers of differentiation as well as decreased replicative potential and tumor growth in vivo.³⁸ To date, no non-nucleoside DNMTi has been tested in a cancer stem cell context. We tested compounds **2** and **5** at different dosages in mouse MbSCs, a cancer stem cell line expressing high levels of DNMTs (Figure S7 in the Supporting Information), to determine their effects on cell proliferation and differentiation. In these assays, compound **5** arrested the MbSC clonogenic activity, induced cell adhesion and differentiation, and impaired significantly the MbSC growth rate, evaluated by both quantifying PCNA levels and MTT assay (Figure 6a,b), whereas **2** was less effective. In MbSCs differentiation

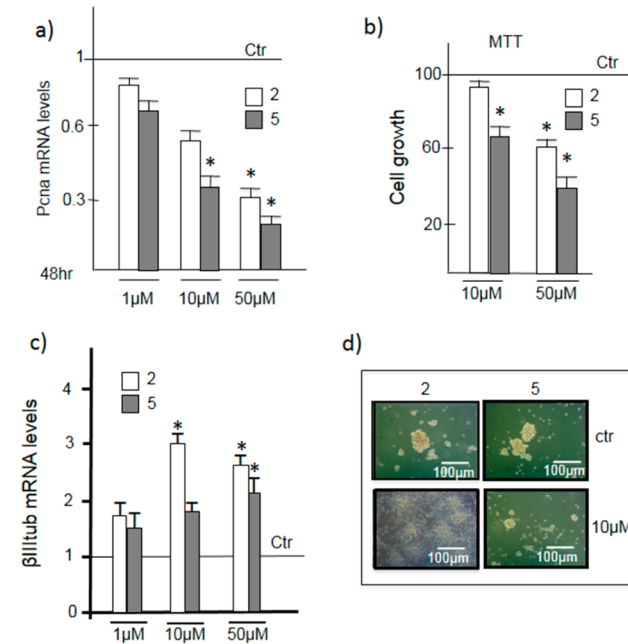


Figure 6. Effects of **2** and **5** in MbSCs. (a) PCNA mRNA levels and (b) MTT assay of MbSCs after 48 h of **2** and **5** treatment or DMSO as control (Ctr). *P < 0.05 versus untreated cells (ctr). (c) mRNA levels of β III-tubulin (β IIItub) in **2**- and **5**-treated MbSCs for 48 h. DMSO was used as control. *P < 0.05 versus untreated cells (ctr). (d) Representative bright-field images of MbSCs after **2** or **5** treatment (48 h, 10 μ M) or DMSO as control.

assays, evaluated by both β III-tubulin RT-PCR and phase-contrast images (Figure 6c,d), **2** showed the highest differentiation effect after treatment with lower doses (10 μ M), whereas **5** required higher concentrations (50 μ M) to reach significance. To the best of our knowledge, **2** and **5** are the first examples of non-nucleoside DNMTi tested in cancer stem cells (CSCs).

CONCLUSIONS

Through chemical manipulation applied on the structure of **1**, we identified compound **5**, a novel non-nucleoside DNMTi more potent than **1** and more selective toward other AdoMet-dependent protein methyltransferases (PRMT1 and GLP). Tested on a panel of cancer cells (leukemia, U937; breast cancer, MDA-MB-231; Burkitt's lymphoma, RAJI; and prostate cancer, PC-3) as well as on PBMCs, compound **5** displayed

comparable activity as **1** and with less toxicity. In MbSCs at 10 μM , **5** significantly blocked proliferation but required higher doses (50 μM) to induce differentiation, whereas related compound **2**, which was less potent as an antiproliferative agent, showed high differentiating activity. The anticancer activity displayed by **2** and **5** in the tested cancer cells, including in cancer stem cells, suggests their use as potent and selective non-nucleoside DNMTi for cancer therapy.

EXPERIMENTAL SECTION

Chemistry. Melting points were determined on a Buchi 530 melting-point apparatus and are uncorrected. ^1H NMR and ^{13}C NMR spectra were recorded at 400 MHz on a Bruker AC 400 spectrometer; chemical shifts are reported in δ (ppm) units relative to the internal reference, tetramethylsilane (Me_4Si). EIMS spectra were recorded with a Fisons Trio 1000 spectrometer; only molecular ions (M^+) and base peaks are given. All compounds were routinely checked by TLC, ^1H NMR, and ^{13}C NMR spectra. TLC was performed on aluminum-backed silica gel plates (Merck DC, Alufolien Kieselgel 60 F254) with spots visualized by UV light. All solvents were reagent grade and, when necessary, were purified and dried by standard methods. Concentration of solutions after reactions and extractions involved the use of a rotary evaporator operating at reduced pressure of ca. 20 Torr. Organic solutions were dried over anhydrous sodium sulfate. Elemental analysis was used to determine the purity of the described compounds, which was found to be >95%. Analytical results are within $\pm 0.40\%$ of the theoretical values. All chemicals were purchased from Aldrich Chimica, Milan (Italy), or from Alfa Aesar, Milan (Italy), and were of the highest purity.

General Procedure for the Synthesis of Ester Intermediates 16a–c and 20 and Nitro Intermediates 17a–c and 18. Example: Synthesis of Ethyl 3-(Quinolin-4-ylamino)benzoate (16b). 4-Chloroquinoline (6.05 mmol, 0.99 g), ethyl 3-aminobenzoate (6.05 mmol, 1 g), and a catalytic amount (4 drops) of 37% hydrochloric acid were refluxed for 2 h. The reaction was allowed to cool to room temperature, and the precipitated solid was filtered off, washed with water (3×5 mL), and recrystallized by methanol to afford pure **16b** as a hydrochloride salt. ^1H NMR ($\text{DMSO}-d_6$, 400 MHz) δ 1.34 (t, 3H, $J = 7.2$ Hz, $-\text{COOCH}_2\text{CH}_3$), 4.36 (q, 2H, $J = 7.2$ Hz, $-\text{COOCH}_2\text{CH}_3$), 6.88 (d, 1H, $J = 5.2$ Hz, quinoline proton), 7.74 (m, 2H, benzene protons), 7.84 (t, 1H, $J = 7.4$ Hz, benzene proton), 8.00 (d, 1H, $J = 8.2$ Hz, quinoline proton), 8.06–8.12 (m, 3H, quinoline and benzene protons), 8.56 (d, 1H, $J = 8.2$ Hz, quinoline proton), 8.81 (d, 1H, $J = 5.2$ Hz, quinoline proton), 11.08 (bs, 1H, $-\text{NH}$), 14.68 (bs, 1H, H^+). ^{13}C NMR ($\text{DMSO}-d_6$, 100 MHz) δ 14.1, 60.9, 112.8, 114.2, 119.9, 121.6, 122.1, 124.2, 125.7, 129.2, 129.6, 130.9, 133.7, 138.7, 142.3, 149.7, 151.6, 165.9. MS (EI) m/z [M] $^+$ calcd for $\text{C}_{18}\text{H}_{16}\text{N}_2\text{O}_2$, 292.1212; found, 292.1218.

General Procedure for the Synthesis of Acid Intermediates 14a–c and 21. Example: Synthesis of 3-(Quinolin-4-ylamino)benzoic Acid (14b). A solution of ethyl 3-(quinolin-4-ylamino)benzoate **16b** (1.71 mmol, 0.5 g) and 2 N KOH (6.84 mmol, 0.38 g) in ethanol (15 mL) was stirred overnight at room temperature. Then, the solvent was evaporated, and 2 N HCl was slowly added until pH 5.0 was obtained. The colorless solid was filtered, washed with water (3×5 mL), and recrystallized from methanol to obtain pure **14b**. ^1H NMR ($\text{DMSO}-d_6$, 400 MHz) δ 7.00 (d, 1H, $J = 5.2$ Hz, quinoline proton), 7.51–7.58 (m, 2H, quinoline and benzene protons), 7.63 (d, 1H, benzene proton), 7.68–7.75 (m, 2H, quinoline and benzene protons), 7.90–7.93 (m, 2H, quinoline and benzene protons), 8.39 (d, 1H, $J = 8.0$ Hz, quinoline proton), 8.51 (d, 1H, $J = 5.2$ Hz, quinoline proton), 9.17 (bs, 1H, NH), 12.0 (bs, 1H, COOH). ^{13}C NMR ($\text{DMSO}-d_6$, 100 MHz) δ 112.8, 119.5 (2C), 120.2, 121.6, 124.2, 125.7, 129.2, 129.6, 131.1 (2C), 138.7, 149.7, 151.1, 151.6, 169.3. MS (EI) m/z [M] $^+$ calcd for $\text{C}_{16}\text{H}_{12}\text{N}_2\text{O}_2$, 264.0899; found, 264.0902.

General Procedure for the Synthesis of Anilines 15a–c, 19, and 13. Example: Synthesis of N^4 -(3-Aminophenyl)-6-methylpyrimidine-2,4-diamine (15b). To a cooled solution of 6-methyl- N^4 -(3-nitrophenyl)pyrimidine-2,4-diamine **17b** (1.63 mmol, 0.5 g) and stannous chloride dihydrate (8.15 mmol, 1.84 g) in ethanol (10 mL) was slowly added a 37% hydrochloric acid solution (0.3 mL) at 0 °C.

The reaction was then kept at 80 °C for 1 h. Afterward, the reaction was quenched at room temperature by a 2 N sodium carbonate solution (20 mL), and the mixture was extracted with ethyl acetate (3×30 mL), washed with brine (3×30 mL), dried with anhydrous sodium sulfate, filtered, and concentrated under reduced pressure. The crude solid was recrystallized from cyclohexane to give the pure product **15b**. ^1H NMR ($\text{DMSO}-d_6$, 400 MHz) δ 2.06 (s, 3H, $-\text{CH}_3$), 4.92 (bs, 2H, $-\text{NH}_2$ -aniline), 5.87 (s, 1H, pyrimidine proton), 5.97 (bs, 2H, $-\text{NH}_2$ -pyrimidine), 6.19 (d, 1H, $J = 8.0$ Hz, aniline proton), 6.80 (d, 1H, $J = 8.0$ Hz, aniline proton), 6.87–6.91 (m, 2H, aniline protons), 8.64 (bs, 1H, $-\text{NH}$). ^{13}C NMR ($\text{DMSO}-d_6$, 100 MHz) δ 23.9, 93.8, 102.7, 105.0, 107.8, 130.3, 143.2, 147.8, 163.1, 164.5, 170.2. MS (EI) m/z [M] $^+$ calcd for $\text{C}_{11}\text{H}_{13}\text{N}_5$, 215.1171; found, 215.1167.

General Procedure for the Synthesis of Compounds 1–12 and 22. Example: Synthesis of N -(3-(2-Amino-6-methylpyrimidin-4-ylamino)phenyl)-3-(quinolin-4-ylamino)benzamide (5). Triethylamine (3.04 mmol, 0.42 mL) and benzotriazol-1-yl-oxytritypyrrolidinophosphonium hexafluorophosphate (PyBOP) (0.91 mmol, 0.47 g) were added to a solution of 3-(quinolin-4-ylamino)benzoic acid **14b** (0.76 mmol, 0.2 g) in anhydrous *N,N*-dimethylformamide (5 mL) under a nitrogen atmosphere. The resulting mixture was stirred for 30 min at room temperature followed by the addition of N^4 -(3-aminophenyl)-6-methylpyrimidine-2,4-diamine **15b** (0.76 mmol, 0.16 g) under a nitrogen atmosphere, and the reaction was stirred overnight. The reaction was quenched with water (50 mL) and extracted with ethyl acetate (3×30 mL). The combined organic extracts were dried, and the residue obtained upon evaporation of solvent was purified by column chromatography (SiO_2 eluting with ethyl acetate/methanol 10:1) to provide pure **5**. ^1H NMR ($\text{DMSO}-d_6$, 400 MHz) δ 2.10 (s, 3H, $-\text{CH}_3$), 5.94 (s, 1H, pyrimidine proton), 6.07 (bs, 2H, $-\text{NH}_2$ -pyrimidine), 7.06 (d, 1H, $J = 4.8$ Hz, quinoline proton), 7.26 (t, 1H, $J = 8.0$ Hz, benzene proton), 7.35 (d, 1H, $J = 7.6$ Hz, quinoline proton), 7.55–7.61 (m, 4H, benzene and quinoline protons), 7.72–7.75 (m, 2H, benzene protons), 7.91 (d, 1H, $J = 8.0$ Hz, quinoline proton), 7.95 (s, 1H, benzene proton), 8.03 (s, 1H, benzene proton), 8.42 (d, 1H, $J = 8.4$ Hz, quinoline proton), 8.52 (d, 1H, $J = 5.6$ Hz, quinoline proton), 9.04 (bs, 1H, $-\text{NH}$ -pyrimidine), 9.16 (bs, 1H, $-\text{NH}$ -quinoline), 10.18 (s, 1H, $-\text{CONH}-$). ^{13}C NMR ($\text{DMSO}-d_6$, 100 MHz) δ 23.9, 93.8, 108.0, 111.6, 111.8, 112.8, 113.4, 117.5, 121.2, 121.6, 124.2, 125.7, 129.2, 129.6, 129.7, 133.9, 135.0, 136.7, 138.7, 142.5, 142.6, 149.7, 151.6, 163.1, 164.5, 164.7, 170.2. MS (EI) m/z [M] $^+$ calcd for $\text{C}_{27}\text{H}_{23}\text{N}_7\text{O}$, 461.1964; found, 461.1969.

N-(4-(2-Amino-6-methylpyrimidin-4-ylamino)phenyl)-4-(quinolin-4-ylamino)benzamide (1, SGI-1027). ^1H NMR ($\text{DMSO}-d_6$, 400 MHz) δ 2.10 (s, 3H, $-\text{CH}_3$), 5.88 (s, 1H, pyrimidine proton), 6.14 (bs, 2H, $-\text{NH}_2$ -pyrimidine), 7.21 (d, 1H, $J = 5.4$ Hz, quinoline proton), 7.48–7.81 (m, 8H, benzene and quinoline protons), 7.93–8.03 (m, 3H, benzene and quinoline protons), 8.42 (d, 1H, $J = 8.4$ Hz, quinoline proton), 8.52 (d, 1H, $J = 5.6$ Hz, quinoline proton), 8.97 (bs, 1H, $-\text{NH}$ -pyrimidine), 9.25 (bs, 1H, $-\text{NH}$ -quinoline), 10.06 (bs, 1H, $-\text{CONH}-$). ^{13}C NMR ($\text{DMSO}-d_6$, 100 MHz) δ 23.9, 93.8, 111.4 (2C), 112.8, 117.7 (2C), 121.6, 122.4 (2C), 124.2 (2C), 125.7, 127.9, 129.2, 129.6, 130.2 (2C), 136.5, 138.7, 149.3, 149.7, 151.6, 163.1, 164.5, 164.7, 170.2. MS (EI) m/z [M] $^+$ calcd for $\text{C}_{27}\text{H}_{23}\text{N}_7\text{O}$, 461.1964; found, 461.1969.

N-(3-(2-Amino-6-methylpyrimidin-4-ylamino)phenyl)-4-(quinolin-4-ylamino)benzamide (2). ^1H NMR ($\text{DMSO}-d_6$, 400 MHz) δ 2.10 (s, 3H, $-\text{CH}_3$), 5.95 (s, 1H, pyrimidine proton), 6.07 (bs, 2H, $-\text{NH}_2$ -pyrimidine), 7.21–7.25 (m, 2H, benzene and quinoline protons), 7.37 (d, 1H, $J = 8.2$ Hz, benzene proton), 7.50–7.61 (m, 4H, benzene and quinoline protons), 7.75 (t, 1H, $J = 7.4$ Hz, quinoline proton), 7.93–8.03 (m, 4H, benzene and quinoline protons), 8.42 (d, 1H, $J = 8.4$ Hz, quinoline proton), 8.52 (d, 1H, $J = 5.6$ Hz, quinoline proton), 9.03 (bs, 1H, $-\text{NH}$ -pyrimidine), 9.25 (bs, 1H, $-\text{NH}$ -quinoline), 10.05 (bs, 1H, $-\text{CONH}-$). ^{13}C NMR ($\text{DMSO}-d_6$, 100 MHz) δ 23.9, 93.8, 108.0, 111.4 (2C), 111.6, 112.8, 113.4, 121.6, 124.2 (2C), 125.7, 129.2, 129.6, 129.7, 130.2 (2C), 136.7, 138.7, 142.6, 149.3, 149.7, 151.6, 163.1, 164.5, 164.7, 170.2. MS (EI) m/z [M] $^+$ calcd for $\text{C}_{27}\text{H}_{23}\text{N}_7\text{O}$, 461.1964; found, 461.1969.

N-(2-Amino-6-methylpyrimidin-4-ylamino)phenyl)-4-(quinolin-4-ylamino)benzamide (3). ^1H NMR ($\text{DMSO}-d_6$, 400 MHz) δ 2.09 (s, 3H, $-\text{CH}_3$), 5.88 (s, 1H, pyrimidine proton), 6.31 (bs, 2H, $-\text{NH}_2$ -pyrimidine),

7.18–7.22 (m, 2H, benzene and quinoline protons), 7.37–7.50 (m, 4H), 7.58–7.65 (m, 2H benzene and quinoline protons), 7.72–7.77 (m, 2H, benzene protons), 7.94–7.96 (m, 2H, quinoline protons), 8.37 (d, 1H, J = 7.6 Hz, quinoline proton), 8.55 (bs, 1H, –NH-pyrimidine), 8.58 (d, 1H, J = 4.8 Hz, quinoline proton), 9.25 (bs, 1H, –NH-quinoline), 10.15 (bs, 1H, –CONH–). ^{13}C NMR (DMSO- d_6 , 100 MHz) δ 23.9, 93.8, 112.8, 116.4, 117.9, 118.8, 118.9, 121.6, 122.8, 124.2, 125.5, 125.7, 126.1, 128.3, 129.2, 129.6, 132.9, 137.9, 138.7, 147.6, 149.7, 151.6, 151.9, 163.1, 164.5, 167.5, 170.2. MS (EI) m/z [M] $^+$ calcd for $\text{C}_{27}\text{H}_{23}\text{N}_7\text{O}$, 461.1964; found, 461.1969.

N-(4-(2-Amino-6-methylpyrimidin-4-ylamino)phenyl)-3-(quinolin-4-ylamino)benzamide (4). ^1H NMR (DMSO- d_6 , 400 MHz) δ 2.08 (s, 3H, –CH₃), 5.87 (s, 1H, pyrimidine proton), 6.10 (bs, 2H, –NH₂-pyrimidine), 7.06 (d, 1H, J = 5.6 Hz, quinoline proton), 7.54–7.74 (m, 9H, benzene and quinoline protons), 7.90 (d, 1H, J = 8.4 Hz quinoline proton), 8.01 (s, 1H, benzene proton), 8.46 (d, 1H, J = 8.4 Hz, quinoline proton), 8.51 (d, 1H, J = 4.0 Hz, quinoline proton), 9.01 (bs, 1H, –NH-pyrimidine), 9.28 (bs, 1H, –NH-quinoline), 10.30 (s, 1H, –CONH–). ^{13}C NMR (DMSO- d_6 , 100 MHz) δ 23.9, 93.8, 111.8, 112.8, 117.5, 117.7 (2C), 121.2, 121.6, 122.4 (2C), 124.2, 125.7, 127.9, 129.2, 129.6, 133.9, 135.0, 136.5, 138.7, 142.5, 149.7, 151.6, 163.1, 164.5, 164.7, 170.2. MS (EI) m/z [M] $^+$ calcd for $\text{C}_{27}\text{H}_{23}\text{N}_7\text{O}$, 461.1964; found, 461.1969.

N-(2-(2-Amino-6-methylpyrimidin-4-ylamino)phenyl)-3-(quinolin-4-ylamino)benzamide (6). ^1H NMR (DMSO- d_6 , 400 MHz) δ 2.05 (s, 3H, –CH₃), 5.86 (s, 1H, pyrimidine proton), 6.23 (bs, 2H, –NH₂-pyrimidine), 7.04 (d, 1H, J = 5.6 Hz, quinoline proton), 7.20 (m, 2H, benzene and quinoline protons), 7.51–7.74 (m, 7H, benzene and quinoline protons), 7.90–7.92 (m, 2H, benzene and quinoline protons), 8.40 (d, 1H, J = 8.4 Hz, quinoline proton), 8.47 (bs, 1H, –NH-pyrimidine), 8.51 (d, 1H, J = 5.4 quinoline proton), 9.11 (bs, 1H, –NH-quinoline), 10.19 (bs, 1H, –CONH–). ^{13}C NMR (DMSO- d_6 , 100 MHz) δ 23.9, 93.8, 111.8, 112.8, 117.5, 118.9, 121.2, 121.6, 122.8, 124.2, 125.5, 125.7, 126.1, 129.2, 129.6, 133.9, 135.0, 137.9, 138.7, 142.5, 147.6, 149.7, 151.6, 163.1, 164.5, 164.7, 170.2. MS (EI) m/z [M] $^+$ calcd for $\text{C}_{27}\text{H}_{23}\text{N}_7\text{O}$, 461.1964; found, 461.1969.

N-(4-(2-Amino-6-methylpyrimidin-4-ylamino)phenyl)-2-(quinolin-4-ylamino)benzamide (7). ^1H NMR (DMSO- d_6 , 400 MHz) δ 2.07 (s, 3H, –CH₃), 5.85 (s, 1H, pyrimidine proton), 6.08 (bs, 2H, –NH₂-pyrimidine), 7.15 (d, 1H, J = 5.4 Hz, quinoline proton), 7.26 (t, 1H, J = 6.8 Hz, quinoline proton), 7.48–7.75 (m, 8H, benzene and quinoline protons), 7.92 (m, 2H, quinoline protons), 8.16 (d, 1H, J = 8.0 Hz, quinoline proton), 8.55 (d, 1H, J = 4.0 Hz, quinoline proton), 8.95 (bs, 1H, –NH-pyrimidine), 10.26 (bs, 1H, –NH-quinoline), 10.41 (bs, 1H, –CONH–). ^{13}C NMR (DMSO- d_6 , 100 MHz) δ 23.9, 93.8, 112.8, 116.4, 117.7 (2C), 117.9, 118.8, 121.6, 122.4 (2C), 124.2, 125.7, 127.9, 128.3, 129.2, 129.6, 132.9, 136.5, 138.7, 149.7, 151.6, 151.9, 163.1, 164.5, 167.5, 170.2. MS (EI) m/z [M] $^+$ calcd for $\text{C}_{27}\text{H}_{23}\text{N}_7\text{O}$, 461.1964; found, 461.1969.

N-(3-(2-Amino-6-methylpyrimidin-4-ylamino)phenyl)-2-(quinolin-4-ylamino)benzamide (8). ^1H NMR (DMSO- d_6 , 400 MHz) δ 2.08 (s, 3H, –CH₃), 5.91 (s, 1H, pyrimidine proton), 6.05 (bs, 2H, –NH₂-pyrimidine), 7.12–7.28 (m, 3H, benzene and quinoline protons), 7.61–7.73 (m, 3H, benzene and quinoline protons), 7.71–7.76 (m, 3H, benzene protons), 7.91–7.96 (m, 2H, benzene and quinoline protons), 8.16 (d, 1H, J = 8.0 Hz, quinoline proton), 8.55 (d, 1H, J = 4.8 Hz, quinoline proton), 9.02 (bs, 1H, –NH-pyrimidine), 10.10 (bs, 1H, –NH-quinoline), 10.40 (bs, 1H, –CONH–). ^{13}C NMR (DMSO- d_6 , 100 MHz) δ 23.9, 93.8, 108.0, 111.6, 112.8, 113.4, 116.4, 117.9, 118.8, 121.6, 124.2, 125.7, 128.3, 129.2, 129.6, 129.7, 132.9, 136.7, 138.7, 142.6, 149.7, 151.6, 151.9, 163.1, 164.5, 167.5, 170.2. MS (EI) m/z [M] $^+$ calcd for $\text{C}_{27}\text{H}_{23}\text{N}_7\text{O}$, 461.1964; found, 461.1969.

N-(2-(2-Amino-6-methylpyrimidin-4-ylamino)phenyl)-2-(quinolin-4-ylamino)benzamide (9). ^1H NMR (DMSO- d_6 , 400 MHz) δ 2.01 (s, 3H, –CH₃), 5.81 (s, 1H, pyrimidine proton), 6.27 (s, 2H, –NH₂-pyrimidine), 7.12–7.24 (m, 4H, benzene and quinoline protons), 7.48 (d, 1H, J = 7.6 Hz, benzene proton), 7.54–7.61 (m, 3H, benzene protons), 7.71–7.76 (m, 2H, benzene and quinoline protons), 7.92–7.97 (m, 2H, benzene and quinoline protons), 8.08 (d, 1H, J = 8.8 Hz, quinoline protons), 8.57 (m, 2H, quinoline and –NH-pyrimidine protons), 10.44 (bs, 1H, –NH-quinoline), 10.57 (bs, 1H, –CONH–).

^{13}C NMR (DMSO- d_6 , 100 MHz) δ 23.9, 93.8, 112.8, 116.4, 117.9, 118.8, 118.9, 121.6, 122.8, 124.2, 125.5, 125.7, 126.1, 128.3, 129.2, 129.6, 132.9, 137.9, 138.7, 147.6, 149.7, 151.6, 151.9, 163.1, 164.5, 167.5, 170.2. MS (EI) m/z [M] $^+$ calcd for $\text{C}_{27}\text{H}_{23}\text{N}_7\text{O}$, 461.1964; found, 461.1969.

4-(Quinolin-4-ylamino)-N-(4-(quinolin-4-ylamino)phenyl)benzamide (10). ^1H NMR (DMSO- d_6 , 400 MHz) δ 6.83 (d, 1H, J = 6.0 Hz, quinoline proton), 7.20 (d, 1H, J = 4.8 Hz, quinoline proton), 7.42 (d, 2H, J = 8.8 Hz, benzene protons), 7.53 (d, 2H, J = 8.4 Hz, benzene protons), 7.60–7.68 (m, 2H, quinoline protons), 7.79 (t, 1H, J = 7.2 Hz, quinoline proton), 7.83 (t, 1H, J = 7.2 Hz, quinoline proton), 7.94–7.97 (m, 4H, benzene and quinoline protons), 8.07 (d, 2H, J = 7.6 Hz, benzene protons), 8.45–8.49 (m, 2H, quinoline protons), 8.57–8.61 (m, 2H, quinoline protons), 9.49 (bs, 1H, –NH-quinoline), 9.82 (bs, 1H, –NH-quinoline), 10.35 (bs, 1H, –CONH–). ^{13}C NMR (DMSO- d_6 , 100 MHz) δ 111.4 (2C), 112.8 (2C), 117.7 (2C), 121.6 (2C), 122.4 (2C), 124.2 (3C), 125.7 (2C), 127.9, 129.2 (2C), 129.6 (2C), 130.2 (2C), 138.7 (2C), 141.5, 149.3, 149.7 (2C), 151.6 (2C), 164.7. MS (EI) m/z [M] $^+$ calcd for $\text{C}_{31}\text{H}_{23}\text{N}_5\text{O}$, 481.1903; found, 481.1908.

4-(2-Amino-6-methylpyrimidin-4-ylamino)-N-(4-(2-amino-6-methylpyrimidin-4-ylamino)phenyl)benzamide (11). ^1H NMR (DMSO- d_6 , 400 MHz) δ 2.09 (s, 3H, –CH₃), 2.13 (s, 3H, –CH₃), 5.86 (s, 1H, pyrimidine proton), 5.95 (s, 1H, pyrimidine proton), 6.10 (bs, 2H, –NH₂-pyrimidine), 6.26 (bs, 2H, –NH₂-pyrimidine), 7.65 (m, 4H, benzene protons), 7.89 (m, 4H, benzene protons), 8.91 (bs, 1H, –NH-pyrimidine), 9.32 (bs, 1H, –NH-pyrimidine), 9.96 (bs, 1H, –CONH–). ^{13}C NMR (DMSO- d_6 , 100 MHz) δ 23.9 (2C), 93.8 (2C), 111.4 (2C), 117.7 (2C), 122.4 (2C), 124.2 (3C), 125.7 (2C), 127.9, 129.2 (2C), 129.6 (2C), 130.2 (2C), 138.7 (2C), 141.5, 149.3, 149.7 (2C), 151.6 (2C), 164.7. MS (EI) m/z [M] $^+$ calcd for $\text{C}_{23}\text{H}_{23}\text{N}_9\text{O}$, 441.2026; found, 441.2023.

N-(4-Aminophenyl)-4-(quinolin-4-ylamino)benzamide (12). ^1H NMR (DMSO- d_6 , 400 MHz) δ 4.91 (bs, 2H, –NH₂-benzene), 6.56 (d, 2H, J = 7.6 Hz, benzene protons), 7.18 (d, 1H, J = 4.8 Hz, quinoline proton), 7.38 (d, 2H, J = 8.4 Hz, benzene protons), 7.46 (d, 2H, J = 8.4 Hz, benzene protons), 7.60 (t, 1H, J = 7.2 Hz, quinoline proton), 7.74 (t, 1H, J = 7.2 Hz, quinoline proton), 7.93 (d, 1H, J = 8.0 Hz, quinoline proton), 7.97 (d, 2H, J = 8.4 Hz, benzene protons), 8.38 (d, 1H, J = 8.4 Hz, quinoline proton), 8.57 (d, 1H, J = 4.4 Hz, quinoline proton), 9.20 (bs, 1H, –NH-quinoline), 9.79 (bs, 1H, –CONH–). ^{13}C NMR (DMSO- d_6 , 100 MHz) δ 111.4 (2C), 112.8, 116.5 (2C), 121.6, 122.4 (2C), 124.2 (2C), 125.7, 127.9, 129.2, 129.6, 130.2 (2C), 138.7, 144.0, 149.3, 149.7, 151.6, 164.7. MS (EI) m/z [M] $^+$ calcd for $\text{C}_{22}\text{H}_{18}\text{N}_4\text{O}$, 354.1481; found, 354.1486.

4-Amino-N-(4-(2-amino-6-methylpyrimidin-4-ylamino)phenyl)benzamide (13). ^1H NMR (DMSO- d_6 , 400 MHz) δ 2.06 (s, 3H, –CH₃), 5.71 (bs, 2H, –NH₂-benzene), 5.85 (s, 1H, pyrimidine proton), 6.08 (bs, 2H, –NH₂-pyrimidine), 6.60 (d, 2H, J = 8.4 Hz, benzene protons), 7.59–7.64 (m, 4H, benzene protons), 7.71 (d, 2H, J = 8.4 Hz, benzene protons), 8.88 (bs, 1H, –NH-pyrimidine), 9.66 (bs, 1H, –CONH–). ^{13}C NMR (DMSO- d_6 , 100 MHz) δ 23.9, 93.8, 114.3 (2C), 117.7 (2C), 122.4 (2C), 124.2, 127.9, 130.2 (2C), 136.5, 151.8, 163.1, 164.5, 164.7, 170.2. MS (EI) m/z [M] $^+$ calcd for $\text{C}_{18}\text{H}_{18}\text{N}_6\text{O}$, 334.1542; found, 334.1545.

Nanoscale DNMT1 Prescreen and HotSpot DNMT Assay. Compounds 1–13 were tested in 10-dose IC₅₀ mode with 2-fold serial dilutions at a starting concentration of 500 μM against human DNMT1 using poly(dI-dC) (0.001 mg/mL) as a substrate in the presence of AdoMet (1 μM) as a cofactor. Control compounds, AdoHcy (S-(S'-adenosyl)-L-homocysteine) and sinefungin, were tested in 10-dose IC₅₀ mode with 3-fold serial dilutions starting at 100 μM .

Protein Purification. The expression and purification of human DNMT1 with an N-terminal deletion of 600 residues (residues 601–1600) and the human DNMT3A2/DNMT3L complex have been described.⁷ Recombinant rat PRMT1²⁷ and the human G9a-like protein (GLP) C-terminal fragment containing both the ankyrin repeats and catalytic SET domain (residues 734–1235; pXC758)²⁹ were purified as described.

DNMT1 Inhibition Assay. For DNMT1, methyl transfer activity inhibition assays were performed in 20 μL reactions containing 4.6 mM [methyl^3H]-AdoMet (10.0 Ci/mmol; PerkinElmer), 1.0 mM DNA

oligonucleotides, 0.2 μ M DNMT1, 1 mM EDTA, and 50 mM Tris-HCl, pH 7.5. The DNA substrates were 36 bp hemimethylated (GAC)₁₂. Enzymes were preincubated with AdoMet and various concentrations of inhibitors for 5 min at 37 °C before the addition of substrate DNA. After a 15 min incubation, the reactions were terminated by the addition of 1% SDS and 1 mg/mL of protease K and heating at 50 °C for 15 min. The reaction mixtures were spotted on DE81 paper circles (Whatman), washed with 5 mL of cold 0.2 M NH₄HCO₃ (twice), 5 mL of deionized water (twice), and 5 mL of ethanol (once). The dried circles were subjected to liquid scintillation counting with Cytoscint scintillant. All curves were fit individually using Origin 7.5 software (OriginLab).

DNMT3A Inhibition Assay. For the DNMT3a2/3L complex, the inhibition assays were performed 20 μ L reactions containing 4.6 mM [methyl-³H]-AdoMet, 1.0 mM DNA oligonucleotides, 0.3 μ M enzyme, 0.5 mM tris(2-carboxyethyl)phosphine (TCEP), 2.5% (v/v) glycerol, and 50 mM Tris-HCl, pH 7.5. The DNA substrates were 28 bp and contained two CpG sites: 5'-ACA GTA CGT CAA GAT CTT GAC GTA CTG T-3' and the complementary strand.

PRMT1 and GLP Inhibition Assays. For histone methylation inhibitions, the assays were performed in 20 μ L reactions containing 4.6 mM [methyl-³H]-AdoMet, 50 μ g/mL histone from calf thymus (Sigma), 12 μ g/mL (0.3 μ M) PRMT1 or 10 μ g/mL (0.17 μ M) GLP, 100 mM KCl, 5 mM dithiothreitol (DTT), and 50 mM Tris-HCl, pH 8.5. Enzymes were preincubated with AdoMet and various concentrations of inhibitors for 5 min at 37 °C (for PRMT1) or 30 °C (for GLP) before the addition of histone substrates. After incubation (6.5 min for PRMT1 or 5 min for GLP), the reactions were terminated by the addition of 20% trichloroacetic acid (TCA, Fisher Scientific). The reaction mixtures were spotted on GF/A paper circles (Whatman) and washed three times with 3 mL of 10% TCA and once with 3 mL of ethanol. The dried circles were subjected to liquid scintillation counting with Cytoscint scintillant. All curves were fit individually using Origin 7.5 software (OriginLab).

Competition Studies. Competition studies were performed on human DNMT1 according to Gros et al.³⁹ Briefly, the reaction was started by the addition of 94.5 nM DNMT1 to a mix containing the tested compound (up to 1% DMSO), an AdoMet/[methyl-³H]-AdoMet mix in a ratio of 3:1 (isotopic dilution 1*:3), and biotinylated DNA duplex in a 10 μ L final volume. In AdoMet competition studies, AdoMet was varied between 0.5 and 15 μ M while DNA was kept at a near-saturating concentration. In DNA competition studies, DNA was varied between 0.1 and 0.6 μ M while AdoMet was kept at a near-saturating concentration. The tested compounds were spanned from IC₁₀ to IC₈₀. For each substrate concentration, the IC₅₀ of the tested compound was calculated by nonlinear regression fitting with sigmoidal dose response (variable slope). The linear regressions of IC₅₀ against [DNA]/K_m^{DNA} or [AdoMet]/K_m^{AdoMet} were displayed only if their slopes were significantly different from 0. Velocity plots were fitted by Michaelis-Menten regression or nonlinear regression fitting with sigmoidal dose response (variable slope). All regressions were performed with GraphPad Prism 4.03.

Molecular Modeling. Prior to docking calculations, Epik software⁴⁰ was used to calculate the most relevant ionization and tautomeric state of compounds **5** and **1**. Then, the Glide program of the Schrödinger package³³ was used to dock these compounds into the two selected DNMT1 X-ray structures (PDB 3SWR, Hashimoto and Cheng, unpublished data, and PDB 3PTA³²). The receptor grid generation was performed for the box with a center in the putative binding sites of the two structures. The size of the box was determined automatically. The extra precision mode (XP) of Glide was used for docking. The ligand scaling factor was set to 1.0. The geometry of the ligand binding site of the complex between **5** (or **1**) and the DNMT1 structures was then optimized. The binding site was defined as **5** (or **1**) and all amino acid residues located within 8 Å from the ligands. All of the receptor residues located within 2 Å from the binding site were used as a shell. The following parameters of energy minimization were used. The OPLS2005 force field was used. Water was used as an implicit solvent, and a maximum of 5000 iterations of the Polak-Ribier conjugate gradient minimization method was used with a convergence threshold

of 0.01 kJ mol⁻¹ Å⁻¹. All complex pictures were rendered employing the UCSF Chimera software.⁴¹

U-937, RAJI, PC-3, MDA-MB-231, and PBM Cellular Assays. U-937 (histiocytic lymphoma), RAJI (Burkitt's lymphoma), PC-3 (prostate cancer), MDA-MB-231 (breast cancer) cell lines were purchased from Deutsche Sammlung für Mikroorganismen und Zellkulturen (DSZM). Cells were cultured in RPMI 1640 (Lonza) supplemented with 10% fetal calf serum (Lonza) and 1% antibiotic-antimycotic (Lonza). Peripheral blood mononuclear cells (PBMCs) were isolated and cultured as previously described.⁴² Cells in exponential growth phase were treated with compounds at the indicated concentrations. Proliferation and viability were assessed by trypan blue exclusion analysis at the indicated time points. Morphological determination of apoptosis and necrosis was performed as described previously.⁴³

Medulloblastoma Cancer Stem Cell (MbSC) Assays and Stem Cell Cultures and Treatments. MbSCs were isolated and cultivated as described.⁴⁴ In detail, MbSCs were isolated from fresh tumor specimens from Ptch1^{+/−}. Cells were obtained after mechanical and enzymatic dissociation and cultured in serum-free DMEM-F12 supplemented with glucose (0.6%), insulin (25 mg/mL), N-acetyl-L-cysteine (60 mg/mL), heparin (2 mg/mL), B27 (1×), EGF (20 ng/mL), and bFGF (20 ng/mL). MbSCs were also treated to differentiate in vitro after withdrawal of EGF/bFGF and addition of differentiating factors (platelet derived growth factor, PDGF) for 48 h. Compounds **2** and **5** were resuspended in DMSO at 1 mM. Cells were treated with increasing concentration of **2** or **5** (1, 10, and 50 μ M) for 48 h, and DMSO was used as control. Unless otherwise indicated, media and supplements were purchased from Gibco-Invitrogen (Life Science), and chemicals were from Sigma-Aldrich (St. Louis, MO).

RNA Isolation and Real-Time qPCR. Total RNA was isolated with Tri-Reagent (Ambion) according to the manufacturer's procedure, and sample quantification was done using a Nanodrop spectrophotometer (Thermo Scientific). The reverse transcription was performed using a high-capacity cDNA reverse-transcription kit (Applied Biosystem), and quantitative RT-PCR analysis of β III-tubulin, PCNA, DNMT1, DNMT3A, and DNMT3B was performed using a TaqMan assay from Lifetech. mRNA expression was analyzed using the ABI Prism 7900HT sequence detection system (Applied Biosystem) with a TaqMan gene-expression assay according to the manufacturer's protocol (Applied Biosystem). Each amplification reaction was performed in triplicate, and the average of the three threshold-cycle values was used to calculate the relative amount of transcripts in the sample (SDS 2.3 software, Applied Biosystem). mRNA quantification was expressed, in arbitrary units, as the ratio of the sample quantity to the calibrator or to the mean values of control samples. All values were normalized to three endogenous controls: β -actin, β 2-microglobulin, and HPRT.

Western Blot Assay. Cells were lysed using RIPA buffer (Tris-HCl, pH 7.6, 50 mM, deoxycholic acid sodium salt 0.5%, NaCl 140 mM, NP40 1%, EDTA 5 mM, NaF 100 mM, sodium pyrophosphate 2 mM) and protease inhibitors. Lysates were separated on an 8% acrylamide gel and immunoblotted using standard procedures. The following antibodies were used: anti-DNMT1 (sc-20701; Santa Cruz Biotechnology), anti-DNMT3a (sc-365769; Santa Cruz Biotechnology), and anti-DNMT3b (sc-10236; Santa Cruz Biotechnology).

MTT Assay. MbSC were treated with 1, 10, and 50 μ M of compound **2** or **5** for 48 h. The growth of drug-treated cells relative to untreated cells was measured by MTT assay. Each sample was measured in triplicates and repeated at least three times.

■ ASSOCIATED CONTENT

S Supporting Information

Chemical and physical data for compounds **1–22**; elemental analyses for compounds **1–13**; molecular modeling studies on **1**; cellular studies (RAJI, MDA-MB-231, PC-3, and PBM cells) for compounds **4**, **10**, and **11**; and expression levels of DNMTs in medulloblastoma stem cells. This material is available free of charge via the Internet at <http://pubs.acs.org>.

AUTHOR INFORMATION

Corresponding Author

*Tel: +39 06 49913392; Fax: +39 06 491491; E-mail: antonello.mai@uniroma1.it.

Author Contributions

□ These authors contributed equally to this work.

Notes

The authors declare no competing financial interest.

ACKNOWLEDGMENTS

This work was supported by FIRB RBFR10ZJQT, FP7 BLUEPRINT/282510, FP7 COST/TD0905, FP7 Marie Curie REDCAT/215009, the Sapienza-IIT Project, Télévie Luxembourg, the Recherche Cancer et Sang Foundation, the Recherches Scientifiques Luxembourg and Een Häerz fir Kriibskrank Kanner associations, and the U.S. National Institutes of Health (GM049245-20 and DK094346-01). X.C. is a Georgia Research Alliance Eminent Scholar. M.S. is supported by the Action Lions "Vaincre le Cancer". C.F. is a recipient of a postdoctoral grant from the Ministère de la Culture, de l'Enseignement supérieur et de la Recherche du Luxembourg. M.D. is supported by a NRF from MEST (Korea for Tumor Microenvironment grant GCRC 2012-0001184), by a Seoul National University research grant, and by the Research Settlement Fund for the new faculty of SNU. P.B.A. is supported by French Région Midi-Pyrénées (Equipe d'Excellence et FEDER).

ABBREVIATIONS USED

AdoMet, S-adenosyl-L-methionine; AdoHcy, S-adenosyl-homocysteine; bFGF, basic fibroblast growth factor; CSCs, cancer stem cells; DMSO, dimethyl sulfoxide; DNMTs, DNA methyltransferases; DNMTi, DNA methyltransferase inhibitors; DTT, dithiothreitol; EDTA, ethylenediaminetetraacetic acid; EGF, epidermal growth factor; GABA, gamma-aminobutyric acid; GLP, G9a-like protein; HPRT, hypoxanthine guanine phosphoribosyl transferase; IDH1, isocitrate dehydrogenase 1; MbSCs, medulloblastoma stem cells; MTT, 3-(4,5-dimethylthiazol-2-yl)-2,5-diphenyltetrazolium bromide; PBMCs, peripheral blood mononuclear cells; PCNA, proliferating cell nuclear antigen; PDB, Protein Data Bank; PDGF, platelet-derived growth factor; Pitx2c, pituitary homeobox 2c; PRMT1, protein arginine methyltransferase 1; PyBOP, benzotriazol-1-yl-oxy-tritypyrrolidinophosphonium hexafluorophosphate; RT-PCR, real-time polymerase chain reaction; SALL4, Sal-like protein 4; SET, Su(var)3-9-enhancer of zeste-trithorax; TCA, trichloroacetic acid; TCEP, tris(2-carboxyethyl)phosphine

REFERENCES

- (1) Arrowsmith, C. H.; Bountra, C.; Fish, P. V.; Lee, K.; Schapira, M. Epigenetic protein families: A new frontier for drug discovery. *Nat. Rev. Drug Discovery* **2012**, *11*, 384–400.
- (2) Foley, D. L.; Craig, J. M.; Morley, R.; Olsson, C. A.; Dwyer, T.; Smith, K.; Saffery, R. Prospects for epigenetic epidemiology. *Am. J. Epidemiol.* **2009**, *169*, 389–400.
- (3) Yoo, C. B.; Jones, P. A. Epigenetic therapy of cancer: Past, present and future. *Nat. Rev. Drug Discovery* **2006**, *5*, 37–50.
- (4) Baylin, S. B.; Jones, P. A. A decade of exploring the cancer epigenome – biological and translational implications. *Nat. Rev. Cancer* **2011**, *11*, 726–734.
- (5) Florean, C.; Schnekenburger, M.; Grandjenette, C.; Dicato, M.; Diederich, M. Epigenomics of leukemia: From mechanisms to therapeutic applications. *Epigenomics* **2011**, *3*, 581–609.
- (6) Ng, H. H.; Bird, A. DNA methylation and chromatin modification. *Curr. Opin. Genet. Dev.* **1999**, *9*, 158–163.
- (7) Hashimoto, H.; Liu, Y.; Upadhyay, A. K.; Chang, Y.; Howerton, S. B.; Vertino, P. M.; Zhang, X.; Cheng, X. Recognition and potential mechanisms for replication and erasure of cytosine hydroxymethylation. *Nucleic Acids Res.* **2012**, *40*, 4841–4849.
- (8) Jurkowska, R. Z.; Jurkowski, T. P.; Jeltsch, A. Structure and function of mammalian DNA methyltransferases. *ChemBioChem* **2011**, *12*, 206–222.
- (9) Gros, C.; Fahy, J.; Halby, L.; Dufau, I.; Erdmann, A.; Gregoire, J. M.; Ausseil, F.; Vispe, S.; Arimondo, P. B. DNA methylation inhibitors in cancer: Recent and future approaches. *Biochimie* **2012**, *94*, 2280–2296.
- (10) Okano, M.; Bell, D. W.; Haber, D. A.; Li, E. DNA methyltransferases Dnmt3a and Dnmt3b are essential for de novo methylation and mammalian development. *Cell* **1999**, *99*, 247–257.
- (11) Daniel, F. I.; Cherubini, K.; Yurgel, L. S.; de Figueiredo, M. A.; Salum, F. G. The role of epigenetic transcription repression and DNA methyltransferases in cancer. *Cancer* **2011**, *117*, 677–687.
- (12) Esteller, M. Epigenetics in cancer. *N. Engl. J. Med.* **2008**, *358*, 1148–1159.
- (13) Heyn, H.; Moran, S.; Esteller, M. Aberrant DNA methylation profiles in the premature aging disorders Hutchinson-Gilford Progeria and Werner syndrome. *Epigenetics* **2013**, *8*, 28–33.
- (14) Pan, K.; Chen, Y.; Roth, M.; Wang, W.; Wang, S.; Yee, A. S.; Zhang, X. HBP1-mediated transcriptional regulation of DNA methyltransferase 1 and its impact on cell senescence. *Mol. Cell. Biol.* **2013**, *33*, 887–903.
- (15) Zhang, X.; Kusumo, H.; Sakharkar, A. J.; Pandey, S. C.; Guizzetti, M. Regulation of DNA methylation by ethanol induces tissue plasminogen activator expression in astrocytes. *J. Neurochem.* [Online early access]. DOI: 10.1111/jnc.12465. Published Online: Oct 1, 2013.
- (16) Matrisciano, F.; Tueting, P.; Dalal, I.; Kadriu, B.; Grayson, D. R.; Davis, J. M.; Nicoletti, F.; Guidotti, A. Epigenetic modifications of GABAergic interneurons are associated with the schizophrenia-like phenotype induced by prenatal stress in mice. *Neuropharmacology* **2013**, *68*, 184–194.
- (17) Kao, Y. H.; Chen, Y. C.; Chung, C. C.; Lien, G. S.; Chen, S. A.; Kuo, C. C.; Chen, Y. J. Heart failure and angiotensin II modulate atrial Pitx2c promotor methylation. *Clin. Exp. Pharmacol. Physiol.* **2013**, *40*, 379–384.
- (18) Nakano, K.; Boyle, D. L.; Firestein, G. S. Regulation of DNA methylation in rheumatoid arthritis synoviocytes. *J. Immunol.* **2013**, *190*, 1297–1303.
- (19) Zheng, Y. G.; Wu, J.; Chen, Z.; Goodman, M. Chemical regulation of epigenetic modifications: Opportunities for new cancer therapy. *Med. Res. Rev.* **2008**, *28*, 645–687.
- (20) Seidel, C.; Florean, C.; Schnekenburger, M.; Dicato, M.; Diederich, M. Chromatin-modifying agents in anti-cancer therapy. *Biochimie* **2012**, *94*, 2264–2279.
- (21) Yang, C. S.; Wang, X.; Lu, G.; Picinich, S. C. Cancer prevention by tea: Animal studies, molecular mechanisms and human relevance. *Nat. Rev. Cancer* **2009**, *9*, 429–439.
- (22) Candelaria, M.; Herrera, A.; Labardini, J.; González-Fierro, A.; Trejo-Becerril, C.; Taja-Chayeb, L.; Pérez-Cárdenas, E.; de la Cruz-Hernández, E.; Arias-Bofill, D.; Vidal, S.; Cervera, E.; Dueñas-Gonzalez, A. Hydralazine and magnesium valproate as epigenetic treatment for myelodysplastic syndrome. Preliminary results of a phase-II trial. *Ann. Hematol.* **2011**, *90*, 379–87.
- (23) Ceccaldi, A.; Rajavelu, A.; Champion, C.; Rampon, C.; Jurkowska, R.; Jankevicius, G.; Sénaud-Beaufort, C.; Ponter, L.; Gagey, N.; Ali, H. D.; Tost, J.; Vriz, S.; Ros, S.; Dauzon, D.; Jeltsch, A.; Guianvarc'h, D.; Arimondo, P. B. C5-DNA methyltransferase inhibitors: From screening to effects on zebrafish embryo development. *ChemBioChem* **2011**, *12*, 1337–1345.
- (24) Halby, L.; Champion, C.; Sénaud-Beaufort, C.; Ajjan, S.; Drujon, T.; Rajavelu, A.; Ceccaldi, A.; Jurkowska, R.; Lequin, O.; Nelson, W. G.; Guy, A.; Jeltsch, A.; Guianvarc'h, D.; Ferroud, C.; Arimondo, P. B. Rapid synthesis of new DNMT inhibitors derivatives of procainamide. *ChemBioChem* **2012**, *13*, 157–165.

- (25) Castellano, S.; Kuck, D.; Viviano, M.; Yoo, J.; López-Vallejo, F.; Conti, P.; Tamborini, L.; Pinto, A.; Medina-Franco, J. L.; Sbardella, G. Synthesis and biochemical evaluation of δ (2)-isoxazoline derivatives as DNA methyltransferase 1 inhibitors. *J. Med. Chem.* **2011**, *54*, 7663–7677.
- (26) Datta, J.; Ghoshal, K.; Denny, W. A.; Gamage, S. A.; Brooke, D. G.; Phiasivongs, P.; Redkar, S.; Jacob, S. T. A new class of quinoline-based DNA hypomethylating agents reactivates tumor suppressor genes by blocking DNA methyltransferase 1 activity and inducing its degradation. *Cancer Res.* **2009**, *69*, 4277–4285.
- (27) Coleman, R. A. Mechanistic considerations in high-throughput screenings. *Anal. Biochem.* **2003**, *320*, 1–12.
- (28) Copeland, R. A.; Horiuchi, K. Y. Kinetics effects due to non specific substrate-inhibitor interactions in enzymatic reactions. *Biochem. Pharmacol.* **1998**, *55*, 1785–1790.
- (29) Zhang, X.; Cheng, X. Structure of the predominant protein arginine methyltransferase PRMT1 and analysis of its binding to substrate peptides. *Structure* **2003**, *11*, 509–520.
- (30) Shinkai, Y.; Tachibana, M. H3K9 methyltransferase G9a and the related molecule GLP. *Gene Dev.* **2011**, *25*, 781–788.
- (31) Chang, Y.; Zhang, X.; Horton, J. R.; Upadhyay, A. K.; Spannhoff, A.; Liu, J.; Snyder, J. P.; Bedford, M. T.; Cheng, X. Structural basis for G9a-like protein lysine methyltransferase inhibition by BIX-01294. *Nat. Struct. Mol. Biol.* **2009**, *16*, 312–317.
- (32) Song, J.; Rechkoblit, O.; Bestor, T. H.; Patel, D. J. Structure of DNMT1-DNA complex reveals a role for autoinhibition in maintenance DNA methylation. *Science* **2011**, *331*, 1036–1040.
- (33) Glide; Schrödinger, LLC: New York, 2008.
- (34) Pradhan, M.; Estève, P. O.; Chin, H. G.; Samaranayake, M.; Kim, G. D.; Pradhan, S. CXXC domain of human DNMT1 is essential for enzymatic activity. *Biochemistry* **2008**, *47*, 10000–10009.
- (35) Jin, B.; Ernst, J.; Tiedemann, R. L.; Xu, H.; Sureshchandra, S.; Kellis, M.; Dalton, S.; Liu, C.; Choi, J. Linking DNA methyltransferases to epigenetic marks and nucleosome structure genome-wide in human tumor cells. *Cell Rep.* **2012**, *2*, 1411–1424.
- (36) Yang, J.; Corsello, T. R.; Ma, Y. Stem cell gene SALL4 suppresses transcription through recruitment of DNA methyltransferases. *J. Biol. Chem.* **2012**, *287*, 1996–2005.
- (37) Habano, W.; Sugai, T.; Jiao, Y. F.; Nakamura, S. Novel approach for detecting global epigenetic alterations associated with tumor cell aneuploidy. *Int. J. Cancer* **2007**, *121*, 1487–1493.
- (38) Turcan, S.; Fabius, A. W.; Borodovsky, A.; Pedraza, A.; Brennan, C.; Huse, J.; Viale, A.; Riggins, G. J.; Chan, T. A. Efficient induction of differentiation and growth inhibition in IDH1 mutant glioma cells by the DNMT Inhibitor Decitabine. *Oncotarget* **2013**, *4*, 1729–1736.
- (39) Gros, C.; Chauvigné, L.; Poulet, A.; Menon, Y.; Aussel, F.; Dufau, I.; Arimondo, P. B. Development of a universal radioactive DNA methyltransferase inhibition test for high-throughput screening and mechanistic studies. *Nucleic Acids Res.* **2013**, *41*, e185.
- (40) Epik, version 2.0; Schrödinger, LLC: New York, NY, 2009.
- (41) Pettersen, E. F.; Goddard, T. D.; Huang, C. C.; Couch, G. S.; Greenblatt, D. M.; Meng, E. C.; Ferrin, T. E. UCSF Chimera – a visualization system for exploratory research and analysis. *J. Comput. Chem.* **2004**, *25*, 1605–1612.
- (42) Schnekenburger, M.; Grandjenette, C.; Ghelfi, J.; Karius, T.; Foliguet, B.; Dicato, M.; Diederich, M. Sustained exposure to the DNA demethylating agent, 2'-deoxy-5-azacytidine, leads to apoptotic cell death in chronic myeloid leukemia by promoting differentiation, senescence, and autophagy. *Biochem. Pharmacol.* **2011**, *81*, 364–378.
- (43) Charlet, J.; Schnekenburger, M.; Brown, K. W.; Diederich, M. DNA demethylation increases sensitivity of neuroblastoma cells to chemotherapeutic drugs. *Biochem. Pharmacol.* **2012**, *83*, 858–865.
- (44) Po, A.; Ferretti, E.; Miele, E.; De Smaele, E.; Paganelli, A.; Canettieri, G.; Coni, S.; Di Marcotullio, L.; Biffoni, M.; Massimi, L.; Di Rocco, C.; Scrpanti, I.; Gulino, A. Hedgehog controls neural stem cells through p53-independent regulation of nanog. *EMBO J.* **2010**, *29*, 2646–2658.